

ANALYSIS OF FIBER/MATRIX INTERFACE DEBONDING IN STEEL FIBER COMPOSITES UNDER TRANSVERSE LOADING

B. Sabuncuoglu¹, S.A. Tabatabaei² and S.V. Lomov³

¹Department of Mechanical Engineering, Hacettepe University, Beytepe, 06800, Ankara, Turkey,
Email: barissabuncuoglu@hacettepe.edu.tr

²Department of Materials Science, KU Leuven, Kasteelpark Arenberg 44, B-3001, Leuven, Belgium
Email: s.ahmad.tabatabaei@gmail.com,

³Department of Materials Science, KU Leuven, Kasteelpark Arenberg 44, B-3001, Leuven, Belgium
Email: stepan.lomov@kuleuven.be

Keywords: micromechanics, debonding, cohesive, finite element

Abstract

Debonding behavior of matrix from fiber is analyzed for steel-fiber composites and compared with conventional composites with carbon and glass fibers. The results of previously conducted tests were used for interface strength properties for blank and surface treated steel surface. According to the results, surface treatment significantly affects the debonding behavior and generates interfaces much better than the ones with glass and carbon composites. However, the polygonal cross-sectional area of steel fibers causes a very sudden debonding at the interface and causes high stresses in the matrix.

1. Introduction

Steel fiber composites have recently become available as a remedy to the low ductile behavior of composites made of conventional fibers such as glass and carbon. In the expense of some additional weight, it was shown that the toughness of these composites can be increased significantly with these fibers [1]. However, due to the high stiffness contrast between polymer matrix and these steel fibers, they are open to high stress concentrations under transverse loading. Previously an increase in the stress concentrations is observed compared to carbon fiber composites and close to the glass fiber ones [2].

In order to prevent the failure of such materials under certain loading conditions, the damage behavior of composites should be predicted in advance to preserve the structural integrity. The critical issue is using appropriate constitutive models for accurate prediction of real physical phenomena. In general, the debonding or delamination of two interfaces are simulated by cohesive zones [3].

In this study, these cohesive zones are defined between fiber and matrix to simulate the debonding behavior in these materials in micro-scale. The onset of damage with cohesive elements in glass and carbon has been simulated for quite some time. In the case of steel fibers, the behavior can be quite different as additional parameters related with steel fiber / polymeric matrix are playing a role. In addition to high stress concentrations, non-circular cross-section of these materials can reveal different damage behavior compared to the conventional fiber-reinforced composites where such fibers are close to circular shape. The analyses are performed with ABAQUS finite element software with special subroutines to implement various material configurations

2. Micro-mechanical Model

In order to investigate the fiber-matrix debonding behavior, fibers and the matrix region are modelled separately making it to be micro-mechanical model. Hexagonal distribution is a widely accepted packing methodology to analyze fiber-matrix interactions [4, 5] and used in this study. Two fiber volume fractions ($vf = 0.4$ and 0.6) are considered as these are the upper and lower production limits in unidirectional composites. In the case of steel fibers, some of the models are generated with hexagonal

cross-section to understand the effect of cross-sectional shape. Transverse loading is applied along one side of the RVE. Examples of models with circular and hexagonal shape are shown in Fig. 1 with the mesh structure and boundary conditions for fiber volume fraction (ν_f)= 0.6.

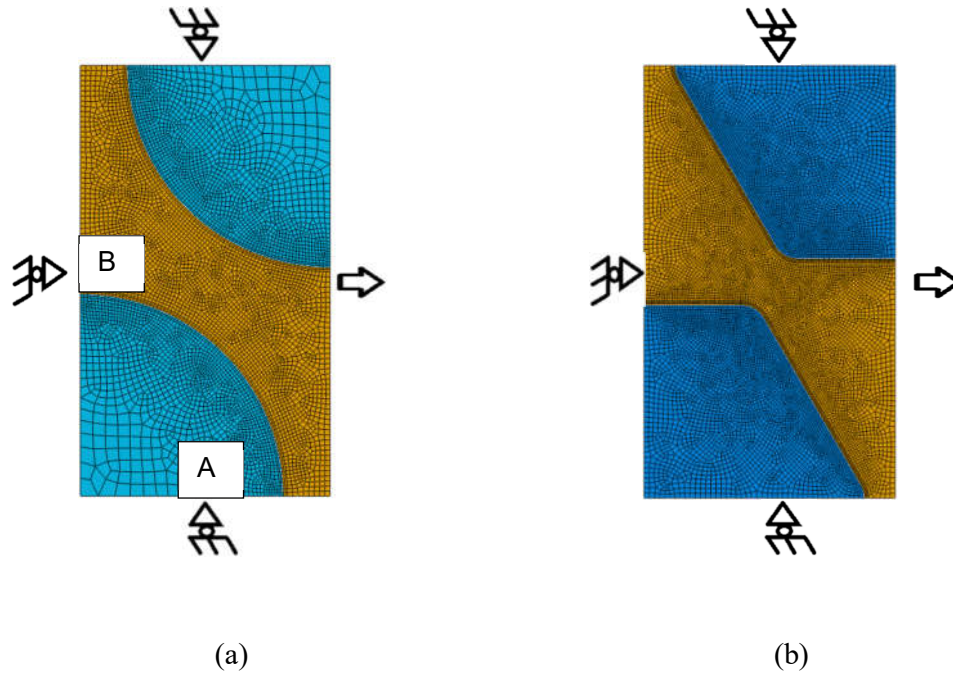


Figure 1. Models with hexagonal packing of fibers with (a) circular, (b) hexagonal cross-sections ($\nu_f = 0.6$)

The models are generated separately for each fiber type with their individual material properties (Table 1). As the conventional diameter of each fiber are different, the dimensions of RVE were scaled according to the diameter of fibers to obtain the same fiber volume fraction for different types of fibers. Epoxy is used as matrix with $E = 3$ GPa and $\nu = 0.4$). Elasto-plastic material properties of epoxy was implemented in tabular form which was obtained from[6].

Table 1. Elastic properties of fibers (d :diameter, E :Young's modulus, ν :Poisson's ratio, L and T : longitudinal and transverse directions, respectively)

Steel	Glass	Carbon (IM-7)
		$E_L = 276$ GPa
$E = 193$ GPa	$E = 72$ GPa	$E_T = 10.3$ GPa
$\nu = 0.3$	$\nu = 0.25$	$G_{TT} = 3.8$ GPa
$d = 30$ μm	$d = 10$ μm	$G_{LT} = 27.9$ GPa
		$\nu_{LT} = 0.26$
		$d = 7$ μm

3. Modelling Of Damage

In cohesive zone approach, when a separation force/displacement is applied, the tractions first increases until a maximum is reached, and then subsequently reduces to zero which results in complete separation (Fig. 2a). Similar curves should be defined for the separation under shear directions and these curves should be combined with a mixed mode behavior (Fig. 2b). The area under the curve is called the fracture energy curve. Sufficient parameters are needed to define these curves. They are presented in Fig. 2c for normal (red) and shear (blue) directions. The part of the curve before maximum load is reached is called the damage initiation and the other side is called the damage evolution zone.

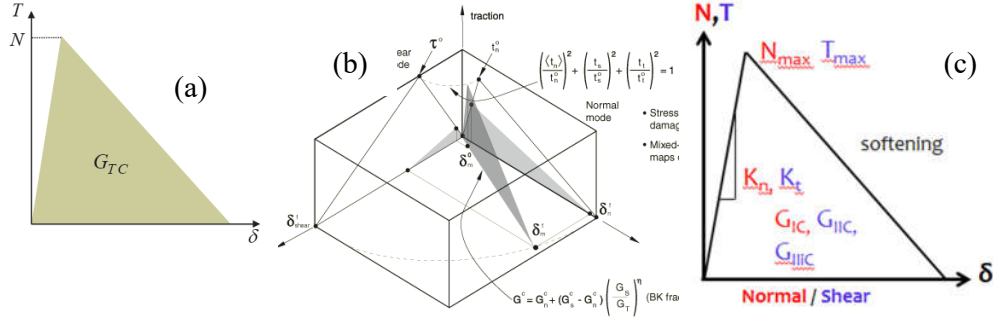


Figure 2. (a) Typical traction-separation curve; (b) Representation of mixed mode traction separation law taken from ABAQUS documentation [7]; (c) Parameters needed to be determined for the analyses

The combined effect of mixed-mode loading can be defined by various formulations. According to the literature, the quadratic traction criteria was found to be the most frequently used method for damage initiation [8-10]. It is given as,

$$\left(\frac{t_n}{N_{max}}\right)^2 + \left(\frac{t_s}{T_{max}}\right)^2 + \left(\frac{t_t}{T_{max}}\right)^2 = 1 \quad (1)$$

Where t_n is the traction along normal direction; t_s and t_t are the tractions along two shear directions. N_{max} and T_{max} are the normal and shear strengths of the interface, respectively, which should be given as input.

For the steel fibers N_{max} is taken from the dolly tests performed for steel-epoxy adhesion [11]. Tests are performed with two configurations. In the first one, epoxy is cured directly on the steel plate whereas in the second one, APS treatment is applied to the surface of fibers. The maximum stresses obtained by these tests are 30 MPa and 63 MPa, respectively. Both of these values are used for analyses in order to observe the difference between these two. Evolution of damage is implemented by linear softening behavior (see Figure 2c) as used similarly in [12-14] for other types of fibers. No data is available for fracture energy between steel fibers and epoxy. In [8], the fracture energy of epoxy is used for epoxy-glass interface as 100 J/m², which is equal to the fracture energy in plane strain conditions for epoxy itself. Same value is used for steel fibers in the study. Trial analyses show that fracture energies around this order do not affect the results significantly.

In order to determine the shear strength (T_{max}), initially, previously performed micro droplet test results were investigated [15]. It was observed that relatively lower strength values are obtained from these tests, which was attributed to the common problems in such tests. The shear strength is suggested to be used 1.5 times the normal strength in [16]. This ratio was observed for both carbon and glass fibers in [8, 9] as well. Therefore, N_{max} values for steel are multiplied by 1.5 and used as T_{max} in this study instead of the results of micro droplet tests. For the penalty stiffness, the value used in [8] (5 e7 MPa/um)

is used after some trial analyses related to convergence. A value of 1×10^{-5} is decided to be used as viscous coefficient in the analyses after some trial analyses.

All the interface properties are given in Table 2 for various models with the model codes used in the further sections of the paper. As an example, a code; S-t-h-0.6 means that a model with hexagonally shaped steel fibers with APS surface treatment and the composite fiber volume ratio of 0.6

Table 2. Material codes for various types of models

Material code	Surface code	Fiber Material	N_{max} (MPa)	T_{max} (MPa)	G_{IC} (J/m ²)	G_{IIC} (J/m ²)	G_{IIIC} (J/m ²)
S	b	Steel (without treatment)	30	45	100	100	100
S	t	Steel (APS treatment)	63	95	100	100	100
G		Glass	50	75	100	100	100
C		Carbon	42	63	280	790	790
Material code	Explanation						
c/h	Circular / hexagonal cross-section						
0.4/0.6	Fiber volume fraction						

4. Results

4.1 Comparison of Steel Fibers with Glass and Carbon Fibers

A stress of 80 MPa is applied to the free point and the results are obtained in every 10 steps. The results are shown in Fig.3 with respect to the applied stress in each step. In this figure, N_{mod} represents the maximum normalized maximum opening distance (the distance between the bottom initially coincident nodes of fiber and matrix) and $CPRESS$ represents the contact pressure at the bottom node. As the traction force is in the direction of separation, pressure is given as negative values. The angle (θ) in Fig 3c is the angle of separation shown in the same figure.

Blank steel gives the maximum opening distance at the same applied stress levels compared to the other fiber types. Low adhesion strength combined with the high stress concentrations results in such behavior. The importance of treating the steel is shown as it gives significantly stronger behavior compared to the other fiber types only in the case of treated steel fiber. The vertical and horizontal lines in Fig 3c and Fig 3d represent the applied stress level when maximum principle stress in the matrix, equal to S_{uts} (75 MPa) is reached at any region of matrix for each model. Up to this point, fiber/matrix debonding is expected but after that, a crack growth towards the inner regions of the matrix is expected. Analysis of Fig 3c shows that in case of blank steel, almost all the matrix is debonded from the fiber until failure in the matrix as the opening angle values reach close to 90°. With the plated steel, strong interface allows a separation of only 25° after which a rupture towards the inside of the matrix is expected.

In Fig 3d, the evolution of maximum principle stresses in the matrix are presented for all models together with the case in which fiber-matrix debonding is prevented (no separation). Apparently, a slight decrease in the evolution of maximum principle stresses can be observed

when debonding starts. These results show that depending on the ultimate tensile strength of the matrix, having a very strong interface does not mean that the part can resist an a larger applied load without damage.

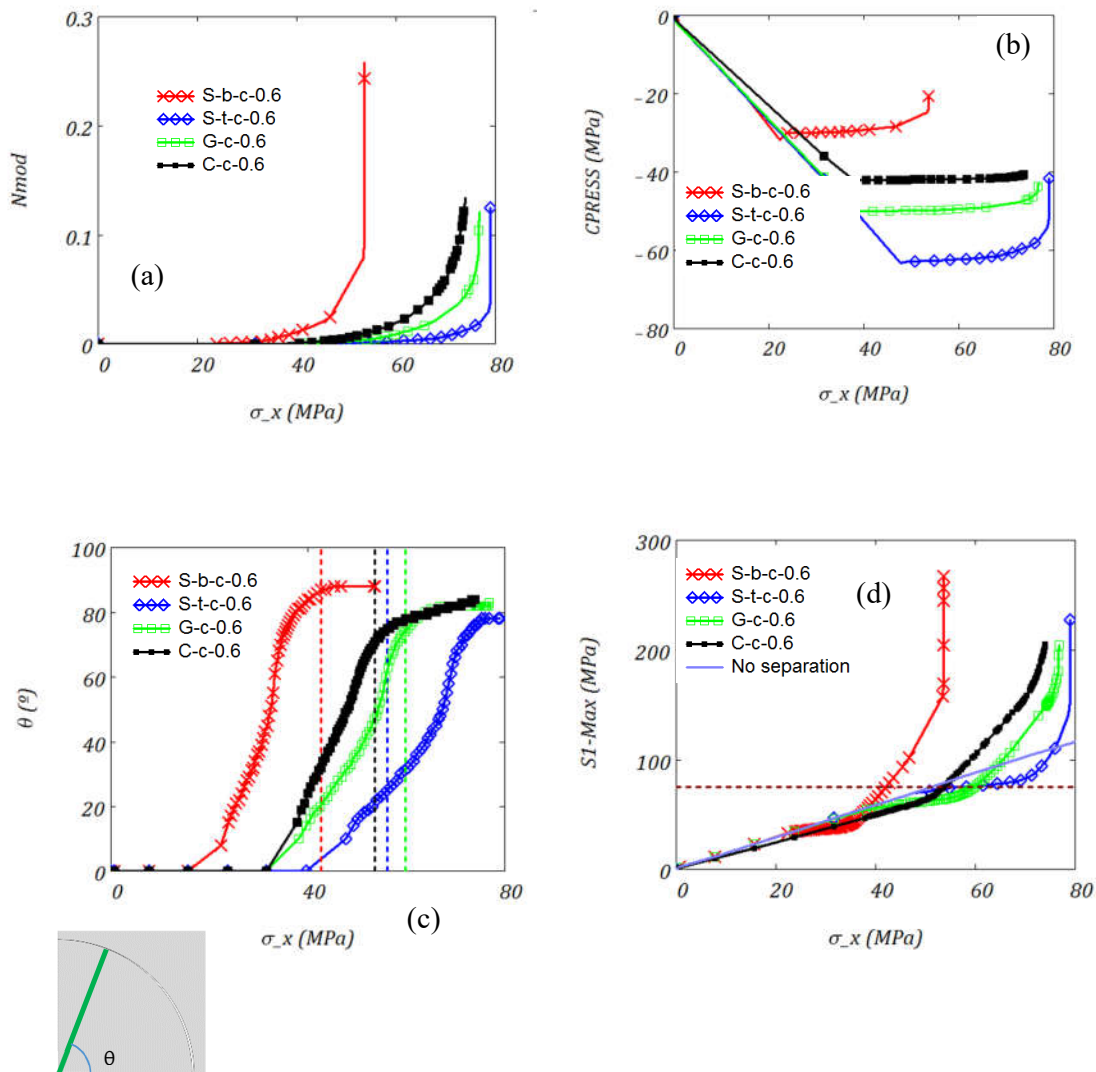


Figure 3. (a) N_{mod} ; (b) $CPRESS$; (c) Opening angle (θ); (d) maximum of maximum principle stress vs applied stress for various types of models

4.2 Effect of fiber cross-section

Steel fibers with hexagonal cross-sections are compared with the circular ones to understand its effect in debonding behavior. The blank and surface treated ones are both investigated. Previously high stress concentrations were observed in hexagonal fibers in [17] under transverse loading. Shown in Fig. 4, this also affects the debonding behavior as the debonding takes place earlier than the corresponding models with fibers having circular cross-sections. Due to the results of Fig. 4b, debonding along one side evolves very rapidly when the crack reaches the straight side of the hexagon. It slows down at the edge, parallel to the load

application direction, as the crack cannot evolve easily. This also gives the indication that the orientation of fibers relative to the loading direction is very important.

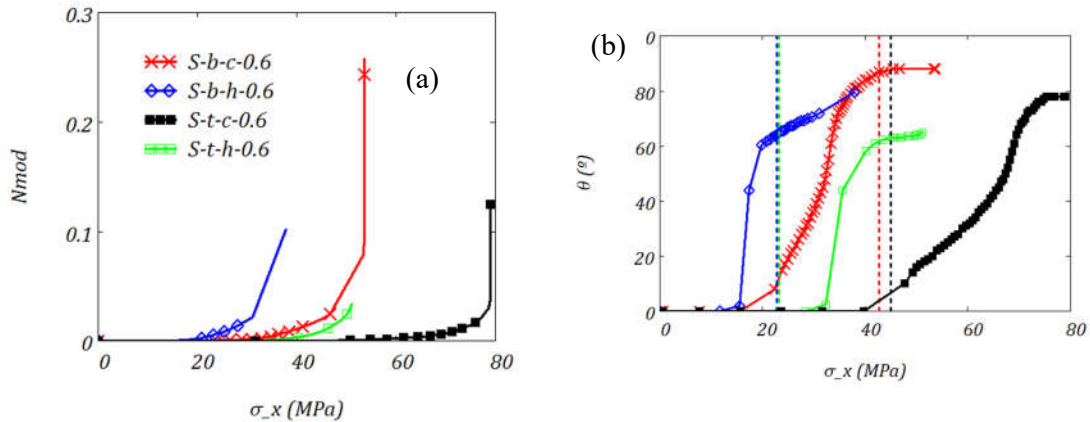


Figure 4. (a) N_{mod} ; (b) θ vs. applied stress for the models with hexagonal and circular fibers

Conclusions

In this study, the debonding behavior of steel fibers are analyzed and compared with the glass and carbon fiber composites. According to the result, the improvement of surfaces of steel fibers with APS treatment significantly reduces the damage encountered due to debonding. With the application of treatment, the debonding behavior of these fibers can perform much better than carbon and glass fibers. However, more detailed analyses should be performed to fully characterize the cohesive interface parameters by performing fiber push in tests for the values of fracture energy and shear strength (T_{max}). A damage model of epoxy should be implemented to link the debonding damage to the damage that would be encountered in epoxy due to the crack propagation. The distribution of fibers are also significantly important that would affect the behavior. A slight decrease in the evolution of maximum principle stress is observed when debonding starts. This shows that debonding can reduce stresses in the matrix in the initial phase of debonding failure. The irregular shape of fibers dominate the debonding behavior similar to findings related to stress concentrations

Acknowledgements

The work reported here was funded by SIM and IWT (Flanders) in the framework of NANOFORCE program (MLM project) and The Scientific and Research Council of Turkey, project number 115C082. S.V. Lomov holds Toray Chair for Composite Materials at KU Leuven, support of which is acknowledged.

References

- [1] M. G. Callens, L. Gorbatikh, and I. Verpoest, "Ductile steel fibre composites with brittle and ductile matrices," *Composites Part A: Applied Science and Manufacturing*, vol. 61, pp. 235-244, 2014.
- [2] B. Sabuncuoglu, S. Orlova, L. Gorbatikh, S. V. Lomov, and I. Verpoest, "Micro-scale finite element analysis of stress concentrations in steel fiber composites under transverse loading," *Journal of Composite Materials*, vol. 49, pp. 1057-1069, April 1, 2015 2014.
- [3] H. Ullah, A. R. Harland, and V. V. Silberschmidt, "Evolution and interaction of damage modes in fabric-reinforced composites under dynamic flexural loading," *Composites Science and Technology*, vol. 92, pp. 55-63, 2014.

- [4] A. R. Maligno, N. A. Warrior, and A. C. Long, "Effects of inter-fibre spacing on damage evolution in unidirectional (UD) fibre-reinforced composites," *European Journal of Mechanics - A/Solids*, vol. 28, pp. 768-776, 2009.
- [5] M. M. Aghdam and A. Dezhsetan, "Micromechanics based analysis of randomly distributed fiber reinforced composites using simplified unit cell model," *Composite Structures*, vol. 71, pp. 327-332, 2005.
- [6] T. Okabe, K. Ishii, M. Nishikawa, and N. Takeda, "Prediction of Tensile Strength of Unidirectional CFRP Composites," *Advanced Composite Materials*, vol. 19, pp. 229-241, 2010/01/01 2010.
- [7] D. Systèmes, "Abaqus 6.11 Documentation," ed, 2011.
- [8] C. G. D.F. Mora, C.S. Lopes, F. Naya, J. Llorca, "Analysis of Transverse Cracking in Unidirectional Composite Plies by Means of Computational Micromechanics," in *16th European Conference on Composite Materials*, Seville, Spain, 2014.
- [9] C. G. F. Naya, C.S. Lopes, S. Van de Veen, J.Llorca, "Combined multi-scale simulations in fiber-reinforced composites," presented at the 16th European Conference on Composite Materials, Seville / Spain, 2014.
- [10] K. Song, C. G. Davila, and C. A. Rose, "Guidelines and Parameter Selection for the Simulation of Progressive Delamination."
- [11] A. K. Ghosh, E. Bertels, B. Goderis, M. Smet, D. Van Hemelrijck, and B. Van Mele, "Optimisation of wet chemical silane deposition to improve the interfacial strength of stainless steel/epoxy," *Applied Surface Science*, vol. 324, pp. 134-142, 1/1/ 2015.
- [12] P. Bhattacharya and T. Siegmund, "The role of glottal surface adhesion on vocal folds biomechanics," *Biomechanics and modeling in mechanobiology*, vol. 14, pp. 283-295, 2015.
- [13] V. I. Kushch, S. V. Shmegeera, and L. Mishnaevsky Jr, "Explicit modeling the progressive interface damage in fibrous composite: Analytical vs. numerical approach," *Composites Science and Technology*, vol. 71, pp. 989-997, 2011.
- [14] S. Li, M. Thouless, A. Waas, J. Schroeder, and P. Zavattieri, "Use of a cohesive-zone model to analyze the fracture of a fiber-reinforced polymer?matrix composite," *Composites Science and Technology*, vol. 65, pp. 537-549, 2005.
- [15] S. Cai, "Study on the interfacial strength of steel fibre poymer composites," MSc. Thesis, Materials Science, KU Leuven, Leuven, 2012.
- [16] S. Ogihara and J. Koyanagi, "Investigation of combined stress state failure criterion for glass fiber/epoxy interface by the cruciform specimen method," *Composites Science and Technology*, vol. 70, pp. 143-150, 2010.
- [17] B. Sabuncuoglu, "On the high stress concentrations in steel fiber composites under transverse loading," *Journal of Reinforced Plastics and Composites*, vol. 33, pp. 1941-1953, 2014.